BMC Ophthalmology

RESEARCH

Open Access

A prognostic model for uveal melanoma in Asian populations: a comparative analysis of clinical features and gene expression patterns using the TRACE and TCGA data

Jingting Luo[1†], Yuning Chen[1†], Zhaoxun Feng[3], Haowen Li[1], Jingying Xiu[1], Yangxu Tao[1], Qiong Yang[1], Yueming Liu[1], Yang Li[1,2*] and Wenbin Wei[1*]

Abstract

Background Uveal melanoma (UM), the most common primary intraocular malignancy in adults, shows racial disparities in incidence, genetic drivers, and clinical outcomes. While most prognostication models are based on Caucasian populations, Asians demonstrate distinct molecular profiles, necessitating population-specific risk stratification.

Methods This study analyzed 53 Asian UM tumors, 17 normal choroidal tissues (TRACE database), and 80 Caucasian UM samples (TCGA database). Differential gene analysis, immune microenvironment profiling, and survival modeling were performed. A 7-gene prognostic signature was developed by LASSO regression and validated across cohorts, with drug sensitivity predicted using GDSC2 data.

Results The Asian UM exhibited 3,827 tumor-specific differentially expressed genes (DEGs) compared to the normal choroid, with enrichment in PI3K-Akt signalling, and 3,814 race-specific DEGs compared to Caucasians, suggesting specific disease pathways and variations in the tumor microenvironment. The tumor microenvironment in Asian UM exhibited increased immunological activation (M1 macrophages, PD-L1, CD8; $p < 0.05$), while Caucasian uveal melanoma was marked by immunosuppressive predominance (M2 macrophages, MDSCs). The seven-gene prognostic model (MMP2, LRAT, NOG, IHH, CDH18, MYH11, and SELE) exhibited strong predictive efficacy in Asians (AUC: 0.979, 0.924, and 0.984 for 1, 3, and 5-year survival) but was less successful in Caucasians. High-risk scores correlated with metastasis (12/26 vs. 4/27; $p = 0.02$) and had independent prognostic value.

Conclusions This cross-racial UM study reveals significant molecular and immune differences, indicating that Asian UM may be more responsive to immunotherapy The population-specific prognostic model improves our

[†]Jingting Luo and Yuning Chen contributed equally to this work.

*Correspondence:
Yang Li
liyangtongren@163.com
Wenbin Wei
weiwenbintr@163.com

Full list of author information is available at the end of the article

understanding of molecular differences in Asian and Caucasian UM, warranting further validation in multiethnic cohorts.

Keywords Uveal melanoma, Racial disparities, Prognostic model, Immune microenvironment

Background

Uveal melanoma (UM) is the most common primary intraocular malignancy in adults [1]. Despite advances in primary tumor treatment, survival rates have not improved, largely due to early subclinical micrometastasis at early stages [2]. Recently, Tebentafusp became the first drug showing a survival benefit in UM patients with metastatic disease confined to HLA: A02-01 [3]. This therapy is expected to be more effective in the adjuvant or early metastatic stages when the disease burden is still low [4]. Therefore, there is a critical need for validated, standardized, and highly accurate prognostic tests to guide surveillance based on metastatic risk and to identify high-risk patients for potential enrollment in adjuvant trials [5]. Moreover, these tests could reduce unnecessary monitoring in low-risk individuals, thereby alleviating test-induced anxiety and lowering healthcare expenses.

Significant differences exist between Asian and Caucasian UM. The incidence is markedly higher in Caucasians (6.02 per million) than in Asians (0.38 per million) [6, 7]. Beyond epidemiological disparities, UM also exhibits ethnic variations in genetic alterations. Mutations in GNAQ and GNA11 occur less frequently in Asian populations (25–60%) compared to Caucasian 80–90%) [8–13], and chromosomal aberrations such as 3p loss and 8q gain have greater prognostic impact in Caucasian UM [14].

UM prognostication has shifted from relying solely on clinical and pathological features, (e.g., tumor size and ciliary body involvement) to incorporating molecular predictors [15, 16]. Gene expression profiling (GEP) has emerged as the gold standard, stratifying UM into Class 1 (low metastatic risk) and Class 2 (high risk), with further subdivisions (e.g., PRAME) offering greater granularity [17, 18]. These classes are derived from the expression level of a predefined panel of genes associated with metastatic potential, typically assessed using microarray or RT-PCR platforms. While commercial GEP assays such as DecisionDx-UM® are widely implemented, their development based predominantly on Caucasian cohorts raises questions about their applicability to non-Caucasian populations [19]. Therefore, establishing population-specific prognostic models to Asian UM patients is critically needed.

This study aims to identify gene expression patterns in Asian UM patients and to construct a predictive model specific for Asian UM. We examined 53 RNA-seq samples from Asian UM patients and 17 healthy controls, creating the most comprehensive gene expression database for Asian UM. We discussed the Cancer Genome Atlas (TCGA) database, which comprises 80 Caucasian UM samples for comparison [17]. We methodically analyzed gene expression profiles between the two cohorts. Our findings provide significant insights into population-specific prognostic markers and may guide personalized management approaches for Asian UM.

Methods

Samples and RNA sequencing

This study adheres to the Helsinki Declaration and has received approval from the Ethics Committee of Beijing Tongren Hospital (Ethics Review Number: TRECKY2018-056). All patients signed informed consent for the use of tissue for research. We obtained 53 UM tumor samples from the patients who underwent local resection surgery or enucleation, all performed by the same ophthalmologist (Dr. Wei) at Beijing Tongren Hospital, China. Additionally, 17 healthy choroidal tissues were obtained from healthy donor (with no ocular diseases) at the Tongren Eye Bank. All 70 samples, along with the patient's clinical characteristics, were registered in the Tongren Ophthalmology Research Association of Clinical Evaluation (TRACE). Each UM patient received comprehensive physical examinations and follow-ups every six months. All collected samples underwent mRNA sequencing and library construction using the Illumina Novaseq6000 sequencing system. We retrieved mRNA sequencing data and corresponding clinical information for 80 UM patients from the TCGA database (https://tcga-data.nci.nih.gov/tcga/).

Different expression gene and enrichment pathway analysis

We utilized count-level RNA-seq data and applied the ComBat function from the sva R package to correct for batch effects. Differentially expressed genes (DEGs) were identified using the "limma" package (version 3.56.2) based on the criteria of $|\mathrm{Log_2FC}| > 2$ and $\mathrm{FDR} < 0.05$. We defined DEG1 as the set of differentially expressed genes obtained by comparing normal choroidal tissues and UM tissues from the TRACE database. DEG2 represents the differentially expressed genes identified by comparing the TRACE-UM and TCGA-UM samples. Gene Ontology (GO) enrichment analysis (including biological process, molecular function, and cellular component) and Kyoto Encyclopedia of Genes and Genomes (KEGG) pathway enrichment analysis were performed using

the "clusterProfiler" package (version 4.8.3) [20]. This R package also conducted Gene Set Enrichment Analysis (GSEA) between groups. Significant enrichment of GO, KEGG, and GSEA pathways was identified using a threshold of p.adjust < 0.05.

Survival analysis

The "survival" package (https://CRAN.R-project.org/package=survival) and "survminer" package (https://CRAN.R-project.org/package=survminer) were used to esti mate overall survival rates for different groups based on the Kaplan-Meier analysis. The log-rank test assessed the statistical significance of survival differences between groups. To evaluate whether Riskscore serves as an independent predictor of patient survival, we performed a multivariate Cox regression analysis. The "timeROC" package [17] was used to generate receiver operating characteristic (ROC) curves and calculate the area under the curve (AUC) values.

Key gene selection and prognostic model construction

The intersection of DEG1 and DEG2 was taken. The functional relationships and interactions of proteins were analyzed using the STRING database (version 11.0) [21]. The key genes within the PPI network were further screened using the CytoHubba plugin in Cytoscape (version 3.7.2) [22] based on maximal clique centrality [23].

To identify genes significantly associated with prognosis, univariate Cox regression analysis was performed on the selected target DEGs with $p < 0.05$, indicating statistical significance. LASSO regression analysis was then conducted using the "glmnet" package [24] to refine the selection of seven prognostically related genes. These selected genes were subsequently used to calculate the risk score for each sample using the following formula:

$$\text{Risk score} = \sum_{i=1}^{n} Coef_i * X_i$$

$Coef_i$ represents the risk coefficient of each gene calculated by the model, and X_i corresponds to its mRNA expression value. Using the selected seven genes (MMP2, LRAT, NOG, IHH, CDH18, MYH11, SELE) along with their regression coefficients, the risk score calculation formula was derived as: Risk score = MMP2*(0.108544590511924) + LRAT*(−0.310767768023121) + NOG*(0.179995401007407) + IHH*(−0.415434021148191) + CDH18*(0.264489286147328) + MYH11*(−0.0520233793170239) + SELE*(−0.435327079973511).

Tumor microenvironment (TME) and drug sensitivity analysis

We used CIBERSORT [25] to calculate the relative proportions of 22 types of immune cells in the samples. The sum of the estimated proportions of all immune cell types in each sample equals 1. The "ESTIMATE" [26] package utilized pre-screened stromal/immune-related gene sets and gene expression data to predict stromal/immune cell infiltration levels in tumor tissue, resulting in stromal and immune scores. Additionally, we estimated the effectiveness of immune checkpoint therapies through the tumor immune dysfunction and exclusion (TIDE) database (http://tide.dfci.harvard.edu/login/), calculating the status of TIDE, myeloid-derived suppressor cells (MDSCs), tumor-associated macrophages M2, expression of interferon-γ (IFN- γ), PD-L1, CD8, and Merck18 for each sample.

For drug sensitivity prediction, we utilized the "oncopredict" package [27]. Using the GDSC2 expression matrix and GDSC2 drug sensitivity data as the training set, we calculated the half-maximal inhibitory concentration (IC_{50}) values of the samples to be predicted based on their expression matrices using the calcPhenotype function.

Other statistical analysis

The Wilcoxon rank-sum test and Pearson correlation analysis were employed in bioinformatic analysis. The student t-test, chi-squared test, and Fisher's exact test were used to analyze the differences in clinical characteristics between the two groups. A $p < 0.05$ was considered statistically significant. All statistical analyses were conducted using R software version 4.3.3.

Results

Tumor-associated differentially expressed genes and clinical characteristics in Asian UM patients

The clinical information of our UM patients (TRACE-UM) is outlined in Supplement Table 1. The average age at diagnosis was 48.11 ± 11.72 years old, with a maximum basal diameter of 15.34 ± 4.12 mm and a height of 11.23 ± 2.61 mm. Most tumors were classified as stage III (AJCC 8th classification), with a predominance of mushroom-shaped tumors; many had subretinal fluid. Approximately half of the tumors invaded the ciliary body. Histologically, the mixed-cell type was the most common, followed by the spindle-cell type.

In comparing normal choroid tissue with UM tissue, we identified 3,827 DEGs (DEG1), most downregulated in the tumor tissue (Fig. 1A). A comparison of the top 20 DEG1 genes based on fold change with clinical features revealed that all deceased patients had stage III tumors and exhibited a higher tendency for ciliary body invasion (Fig. 1B). PRAME, as a key biomarker associated with

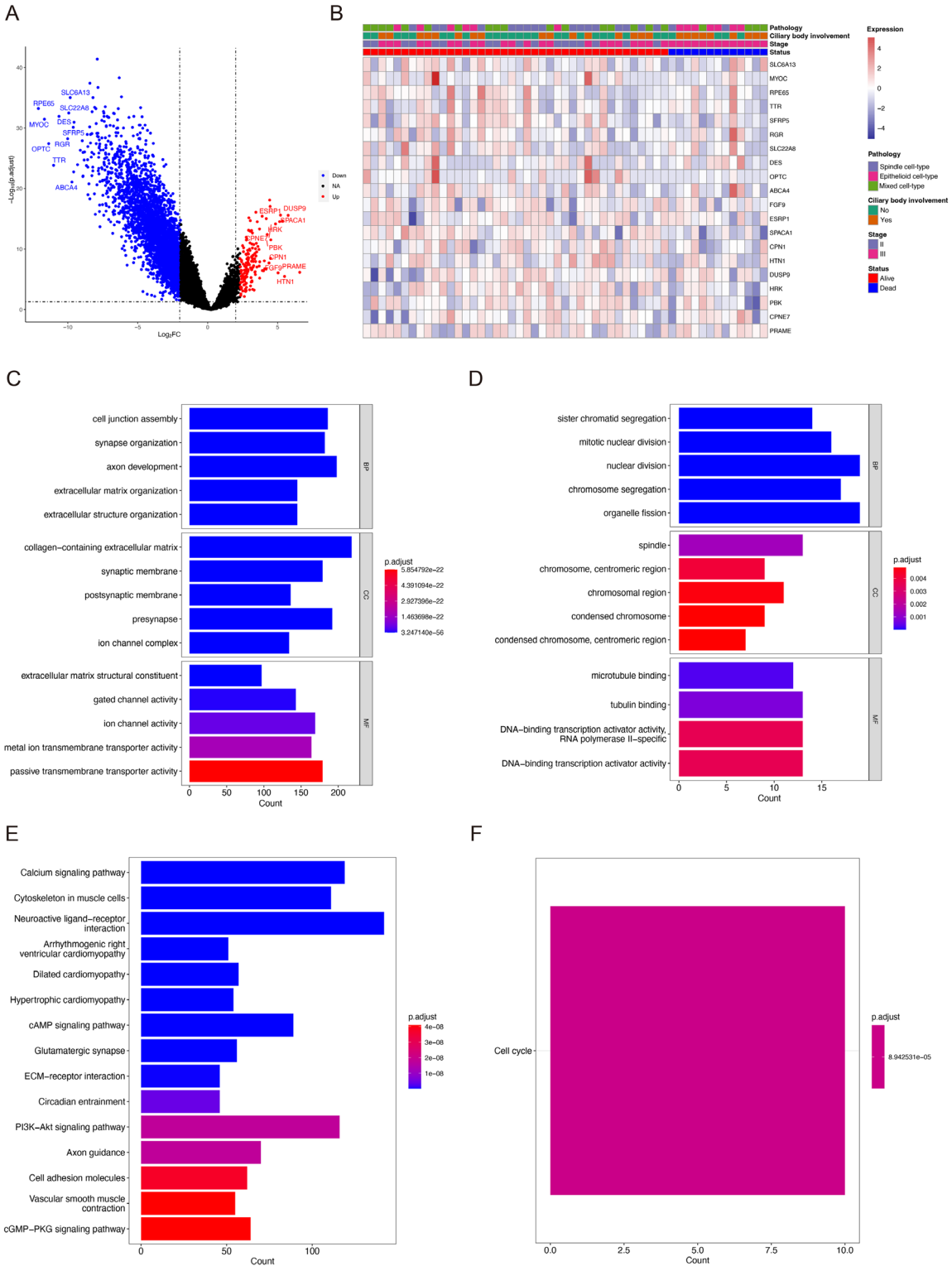

Fig. 1 Tumor-associated differentially expressed genes and clinical characteristics in Asian UM patients. (**A**) Volcano plot of DEGs in TRACE-UM comparing tumor to normal choroid tissue. The horizontal axis represents the Log_2FC of differential expression, and the vertical axis represents -Log_{10} (p.adjust). Red dots indicate upregulated genes, and blue dots indicate downregulated genes. (**B**) Heatmap of the top 20 differentially expressed genes and clinical features. (**C**) GO enrichment analysis for high expressed genes in DEG1. (**D**) GO enrichment analysis for low expressed genes in DEG1. (**E**) KEGG enrichment analysis for high expressed genes in DEG1. (**F**) KEGG enrichment analysis for low expressed genes in DEG1

poor prognosis in UM, was significantly correlated with advanced stage UM in the TRACE cohort ($p = 0.015$). In contrast, high expression levels of SPACA1 and HRK were associated with better survival outcomes ($p = 0.002$ and $p = 0.03$, respectively) (Supplement Table 2).

Subsequently, we conducted GO and KEGG enrichment analysis on DEG1. The results indicated that genes highly expressed in Asian UM primarily involve cell-cell interactions, extracellular matrix regulation, and ion channel functionalities (Fig. 1C). In contrast, genes highly expressed in normal choroid tissue were predominantly associated with cell proliferation processes (Fig. 1D). UM-expressed genes appeared to regulate tumorigenesis and progression through signaling pathways such as PI3K-Akt, calcium, and cGMP-PKG signaling pathways (Fig. 1E). In contrast, normal choroid expressed genes related to the cell cycle (Fig. 1F).

Differences in clinical characteristics and gene expression patterns between Asian and Caucasian UM patients

We compared the clinical characteristics of 53 Asian UM patients from TRACE-UM and 80 Caucasian UM patients from the TCGA (TCGA-UM). Significant differences were observed in age (48.11±11.72 vs. 61.65 ± 13.95 years, $p < 0.001$), tumor size (T-stage, $p = 0.03$), clinical stage ($p = 0.02$), and pathological subtype distribution ($p = 0.002$). TRACE-UM patients also had longer overall survival (44.85±27.39 vs. 27.09 ± 18.42 months, $p < 0.001$) (Supplement Table 3).

After performing batch effect correction, we conducted a DEG analysis on tumor tissues from the TCGA-UM and TRACE-UM, identifying 3,814 DEGs (named DEG2) (Fig. 2A). We classified DEG2 into five gene clusters using the K-Means method based on their relative expression levels (Fig. 2B-C). Genes in clusters C1 and C3 were highly expressed in TRACE tumor samples and were primarily associated with neurodevelopment, cell signal transduction, tumor progression, and immune function regulation. In contrast, clusters C2 and C4 displayed similar expression patterns, with relatively low expression in TRACE tumor samples. Cluster C5 had low expression in both TRACE and TCGA tumor samples. These clusters are mainly related to neural conduction, protein, and lipid metabolism (Fig. 2D).

Association between racial differences and TME with immune therapy response in UM patients

Given the critical role of TME in tumor development, we explored whether there are racial differences in UM TME. By analyzing 22 types of immune infiltrating cells in Asian and Caucasian individuals (Fig. 3A), we found that in Asians, UM exhibited higher enrichment of eosinophils, macrophages M1, monocytes, activated NK cells, and neutrophils. In contrast, Caucasian UM exhibited more macrophages M0, macrophages M2, and T follicular helper cells (Fig. 3B).

Additionally, Asian UM had a significantly higher ESTIMATE score, stromal score, and immune score than Caucasians (Fig. 3C–E), while Caucasian UM showed significantly higher tumor purity (Fig. 3F).

Since the immune landscape of tumors is crucial for patient prognosis and treatment response [28], we further investigated whether racial differences impact the immune landscape of UM. TIDE-related analyses revealed that Asian UM exhibited higher TIDE scores and elevated expression of immune activity-related factors, such as PD-L1, Merck18, CD8, and INF-γ, which were higher than those in Caucasians (Supplement Fig. 1A). Meanwhile, Caucasian UM displayed higher levels of MDSCs and tumor-associated macrophages M2 (Supplement Fig 1B), indicating a higher degree of immune suppression.

Analysis of immune checkpoint receptors and their ligands showed that Asian UM exhibited high expression of checkpoint receptors such as CTLA4, BTLA, TNFRSF18, PDCD1, TIGIT, TNFRSF4, CD86, HAVCR2, and CD40 (Fig. 3G). The ligands exhibiting high expression included FGL1, CD40LG, TNFSF14, TNFSF4, CD86, PD-L1, LGALS9, SNCA, PVR, and HMGB1 (Fig. 3H).

Finally, we compared drug sensitivity (IC_{50}) for commonly used anticancer drugs between Asian and Caucasian UM. Significant differences in IC_{50} were observed for 143 drugs. We visualized the drugs that had lower IC_{50} values (< 50) and in which the IC_{50} for Asian UM was lower ($p < 0.0001$). We chose the top 10 drugs for visualizations (Supplement Fig 1C).

Identification of key genes associated with the oncogenesis and progression of UM in Asian populations and the prognostic risk signature for Asian UM

We identified 150 key candidate genes by analyzing the intersection of DEG1 and DEG2, applying the $|Log_2FC| > 4$, $FDR < 0.05$ criterion through maximal clique centrality analysis (Supplement Table 4). We identified seven prognostically significant genes in UM using univariate Cox regression analysis and LASSO regression. (Fig. 4A). The formula for the risk score was described in the Method section.

Based on the median risk score, TRACE samples were categorized into a high-risk group (26 samples) and a low-risk group (27 samples). Survival analysis revealed that patients in the high-risk group had significantly poorer survival outcomes (Supplement Fig. 2A). ROC curves analysis demonstrated strong predictive performance with AUC values of 0.979, 0.924, and 0.984 for 1-, 3-, and 5-year predictions, indicating the model's effectiveness in forecasting prognosis in Asian UM patients (Fig. 4B).

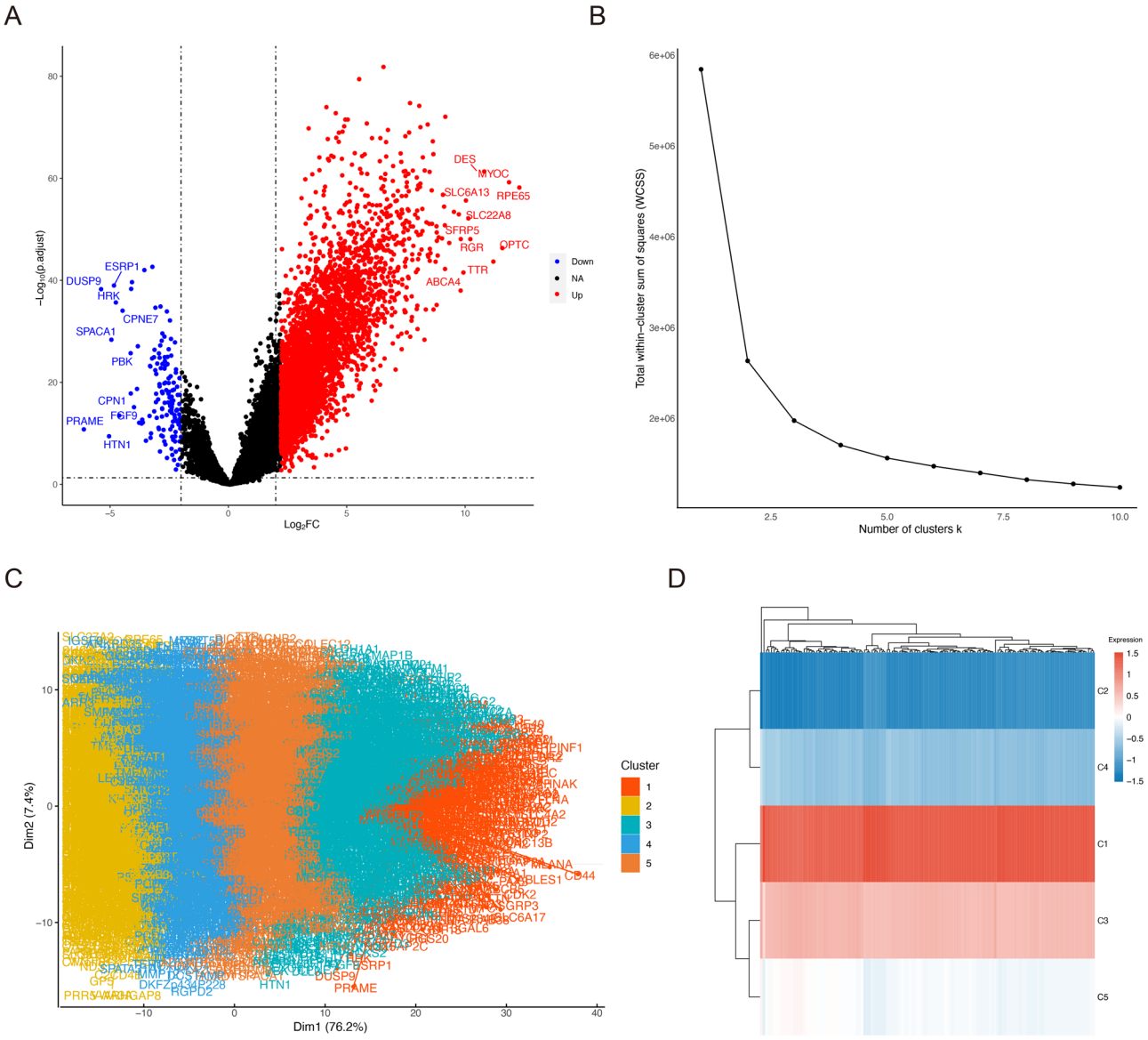

Fig. 2 The differences in gene expression patterns between Caucasians and Asians. (**A**) Volcano plot of DEGs between Caucasians and Asians. The horizontal axis represents Log_2FC of differential expression, and the vertical axis represents $-Log_{10}$ (p.adjust). Red dots indicate upregulated genes compared to Caucasian UM, while blue dots indicate downregulated genes. (**B**) Elbow plot for selecting the optimal K value in K-means clustering. The horizontal axis represents the K value, and the vertical axis represents the within-cluster sum of squares for different K values. (**C**) Visualization of clustering results. (**D**) Heatmap of expression across different samples for different clusters. The horizontal axis represents different samples, and the vertical axis represents different clusters. The red bar indicates relatively high expression, and the blue bar shows relatively low expression

In addition, we analyzed the association between different groups and UM metastasis status (Table 1). A significantly higher number of in the high-risk group had metastasis ($n = 12$), whereas the majority of patients in the low-risk group did not develop metastasis ($n = 23$) ($p = 0.02$).

Further analysis of the expression levels of seven prognostic-related genes in TRACE-UM samples revealed that IHH, MYH11, LRAT, and SELE were highly expressed in the low-risk group. In contrast, the NOG gene was highly expressed in the high-risk group (Fig. 4C). Applying the prognostic model derived from TRACE to the TCGA dataset showed that it could predict the prognosis of Caucasian UM patients, though with lower performance compared to Asian patients (Supplement Fig. 2B–D). Furthermore, we analyzed the impact of individual genes among the seven key genes on UM patient prognosis. High expression of the CDH18 gene was associated with poorer survival (Supplement Fig. 3A, $p = 0.011$), whereas high expression of the MYH11 gene correlated with better prognosis (Supplement Fig. 3B, $p = 0.03$). However, the predictive power of CDH18 and MYH11 alone was weaker

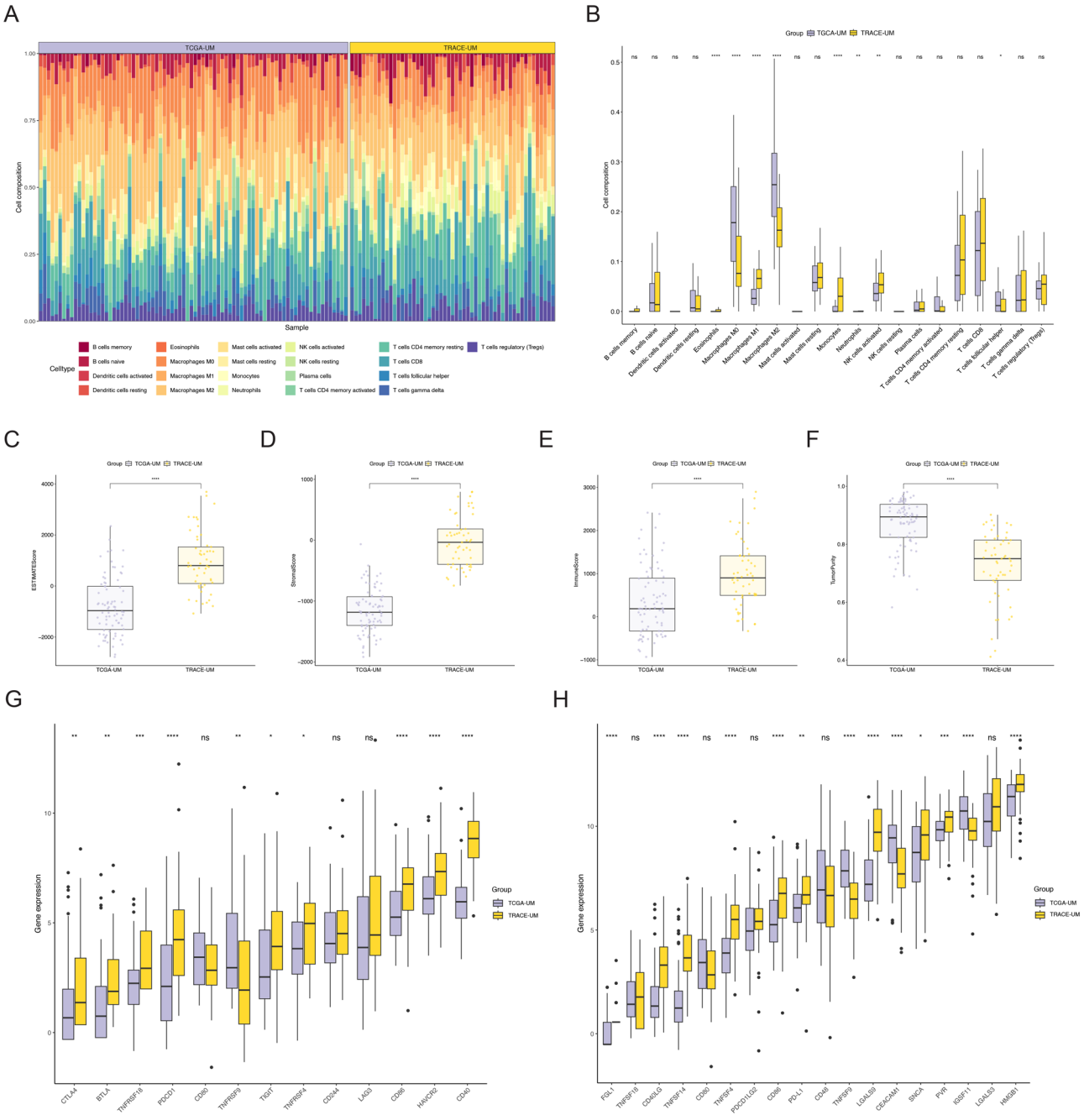

Fig. 3 TME and immune checkpoint analysis between caucasians and Asians. (**A**) The relative abundance of 22 types of immune infiltrating cells in both Caucasian and Asian UM tumor tissue. The horizontal axis represents all samples, and the vertical axis represents relative abundance. Each color represents a different type of immune infiltrating cell. (**B**) The differences in immune cell infiltration between Caucasians and Asians for the 22 types of immune infiltrating cells. The vertical axis represents the relative infiltration proportions of different immune cells. Asterisks (*) indicate significant differences. * $p < 0.05$; ** $p < 0.01$; *** $p < 0.001$. (**C-F**) Boxplot of estimate score (**C**), immune score (**D**), stromal score (**E**), and tumor purity (**F**) between Caucasians and Asians. Every dot indicates one sample, the central box represents the interquartile range, and the line inside the box indicates the median of the dataset. Asterisks (*) indicate significant differences. **** $p < 0.0001$. (**G-H**) Differences in immune checkpoint receptors (**G**) and ligands (**H**) among different ethnicities. Asterisks (*) indicate significant differences. * $p < 0.05$; ** $p < 0.01$; *** $p < 0.001$; **** $p < 0.0001$

than the comprehensive risk score (Supplement Fig. 2A, $p < 0.0001$). These findings support the prognostic risk signature and its potential clinical relevance in predicting outcomes for Asian UM patients.

We performed univariate Cox regression analysis on the clinical characteristics of patients from TRACE and identified three prognosis-related factors: the largest basal diameter, tumor location, and pathology type.

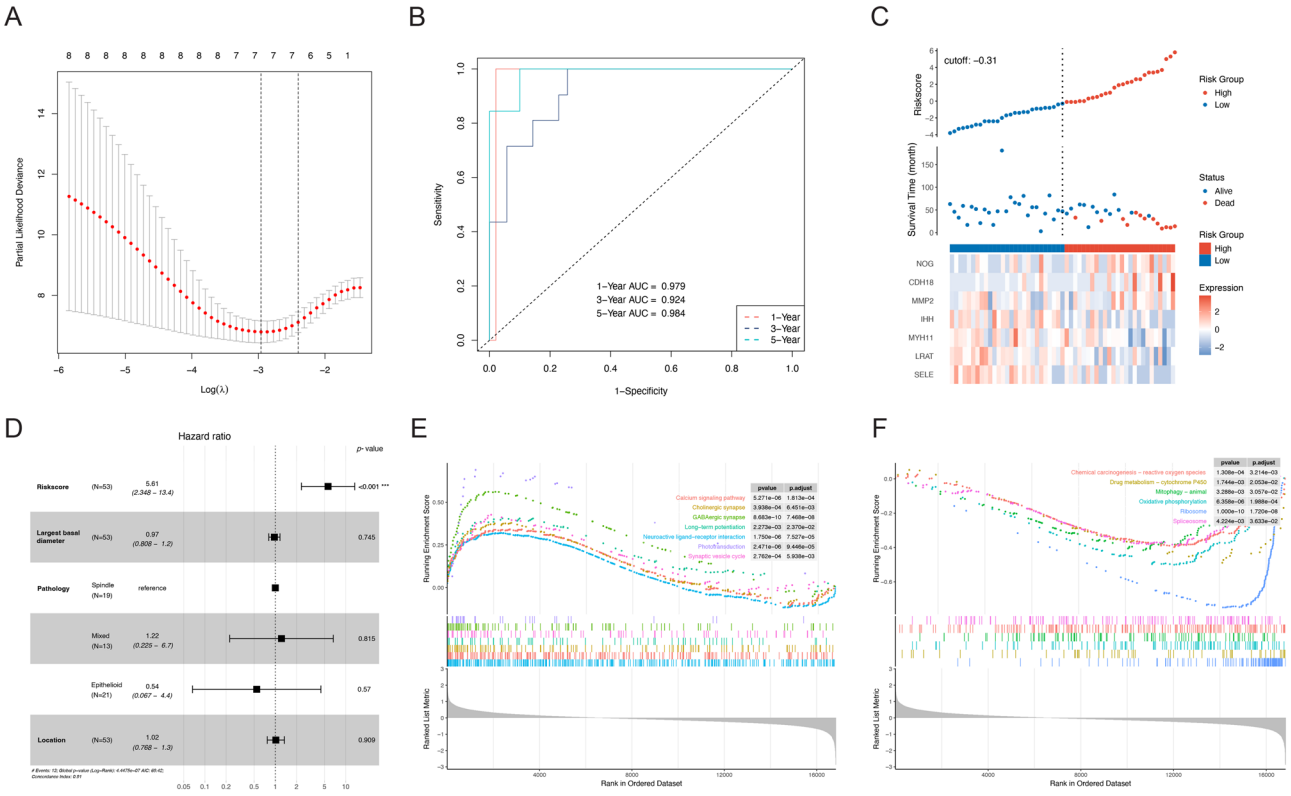

Fig. 4 Establishment of prognostic risk signatures in Asians with UM. (**A**) LASSO regression cross-validation curve. The x-axis represents the value of the regularization parameter, and the y-axis shows the likelihood of deviance. (**B**) ROC curve of the prognostic prediction model for TRACE-UM patients. The x-axis represents the false positive rate and specificity; the y-axis represents the true positive rate and sensitivity. AUC represents the accuracy of the prediction model. (**C**) Risk factor triad diagram from trace. Upper: samples are arranged according to their risk scores, with a cutoff value of −0.31. Middle: the patients' survival time corresponding to each sample is shown. Lower: expression levels of the seven genes used to construct the risk score signature in different samples. (**D**) Forest plot of multivariate regression model. (**E**) Enrichment plot of significantly enriched GSEA pathways in the high-risk group. (**F**) Enrichment plot of significantly enriched GSEA pathways in a low-risk group

Table 1 Different risk groups from TRACE-UM and the occurrence of metastasis

Risk Group	Metastasis Status		Total	*p*-value
	Metastasis	Non-metastasis		
High-Risk	12	14	26	**0.02**
Low-Risk	4	23	27	
Total	16	37	53	

Incorporating these factors into a multivariate regression model confirmed that the risk score is an independent prognostic factor for UM ($p < 0.05$) (Fig. 4D).

GSEA revealed significant differences in 42 pathways between the risk groups. Specifically, gene sets related to neural signal conduction, phototransduction, and ion channels were expressed at higher levels in the high-risk group (Fig. 4E). In contrast, gene sets associated with cell metabolism and oxidative phosphorylation were more highly expressed in the low-risk group (Fig. 4F). Lastly, a statistical comparison of clinical characteristics between high- and low-risk groups revealed significant differences in the largest basal diameter and pathology (Supplement Table 5).

Discussion

This study presents a comprehensive comparative analysis of UM in Asian and Caucasian patients, highlighting variations in gene expression, immune microenvironment, and potential therapeutic responses. To ensure valid cross-cohort comparisons, we applied ComBat normalization to correct batch effects in RNA sequencing data from the TRACE (Asian) and TCGA (Caucasian) cohorts. Our analysis revealed substantial molecular and immune-related disparities that could influence the prognosis and treatment strategies of UM. Critical signaling pathways, including PI3K-Akt, MAPK, and Ras, all of which regulate malignant tumor progression, were predominantly enriched in key genes associated with UM development in Asian populations. Compared to Caucasians, Asian UM patients demonstrated a higher level of immune cell infiltration and increased expression of immune checkpoint receptors and ligands. These findings suggest that population-specific molecular and immune characteristics may influence response to therapy. Furthermore, we detected differential expression of critical genes, including MMP2, LRAT, NOG, IHH,

CDH18, MYH11, and SELE, which can potentially function as biomarkers for prognosis in Asian UM.

Functional enrichment analysis of 150 candidate genes identified the biological processes and important pathways between Asian and Caucasian UM patients, highlighting enrichment in the PI3K-Akt, MAPK, and Ras signaling pathways. The differential activation of these pathways in Asian UM may enhance immune infiltration, while their regulation in Caucasian UM seems to promote immune evasion. Mutations in GNAQ or GNA11 usually generate UM, activating subsequent signaling pathways. Key pathways such as PI3K/AKT, PKC/MAPK/ERK/MEK, and RAS-associated domain family 1 isoform A have been identified as potential therapeutic targets for UM [29–31]. In vitro, several inhibitors targeting these pathways, such as everolimus (mTOR), selumetinib (MAPK), trametinib (MAPK), and the alkylphosphocholine erufosine (PI3K), and the alkylphosphocholine erufosine (PI3K), have demonstrated favourable outcomes [32, 33]. However, clinical trials using these targeted drugs in Caucasian UM patients have yielded unsatisfactory results. Our results suggest that Asian UM patients may exhibit a different pathway activation pattern, affecting their response to targeted therapy. This highlights the need for additional research on treatment strategies for specific populations to improve clinical outcomes.

This study also showed significant differences in the immune microenvironment of UM between Asians and Caucasians. Asian patients showed stronger inflammatory immune response, with extensive infiltration of eosinophils, M1 macrophages, activated NK cells and neutrophils, and high expression of immune checkpoint genes such as PD-L1, CD8, and IFN-γ. In addition, the increased TIDE scores of Asian patients suggest a higher likelihood of a positive response to immunotherapy [34]. Prior studies have linked M1 macrophages and NK cells to more robust anti-tumor immune responses [35], which may account for the superior clinical prognosis observed in Asian patients. Furthermore, larger tumors in the TRACE cohort may contribute to the increased immune infiltration observed, as inflammatory cytokine and chemokine levels correlate with tumor size [36, 37]. A differential upregulation of genes associated with IFN-γ was observed in pre-treatment tumors of patients who responded to immune checkpoint therapy [38]. Furthermore, the expression of PD-L1 was induced in all UM cell lines by treating UM cell lines with IFN-γ [39]. These findings indicate that immune check inhibitors may be particularly effective in Asian UM patients and warrant further clinical validation.

Conversely, Caucasian UM patients exhibited a more immunosuppressive TME dominated by M2 macrophages and MDSCs, which promote tumor immune escape through the secretion of immunosuppressive cytokines such as IL-10 and TGF-β [40, 41]. M2 macrophages are linked to poor prognosis [26] and have been employed to create prognostic models [41]. The immune evasion mechanisms of UM are significantly influenced by the elevated expression of immune checkpoints, including PD-1 and PD-L1, as well as T cell exhaustion [42]. Previous research has demonstrated that PD-1+ infiltrating T cells and PD-L1+ tumor cells are typically expressed at low levels in Caucasian cohorts, irrespective of whether the UM is primary or metastatic [43]. This could explain the relatively low efficacy of immune checkpoint inhibitors in UM. Research suggests that the effectiveness of immunotherapy in Caucasian patients may be enhanced by targeting M2 macrophages or MDSCs [44]. The immune response may differ among various populations, underscoring the necessity of personalized treatment strategies that focus on specific immune microenvironments. Future research will prioritize customizing immunotherapy strategies to the distinctive immune landscapes of individual patient populations.

GEP classification is extensively used in clinical practice across North America [45]. It divides UM patients into low-risk (Class 1) and high-risk (Class 2), facilitating individualized monitoring and treatment strategies (e.g., priority for clinical trials) to enhance resource distribution [46]. The GEP15 platform provides dependable molecular profiling of fine-needle aspiration biopsy specimens [47], with its clinical validity confirmed through multicenter prospective trials [18]. Because GEP15 was developed and validated in North American and European cohorts [48]. Our analysis showed that although GEP15 showed some prognostic value (KM curve $p = 0.014$), its performance was modest, with AUC values of 0.69–0.77 for 1-, 3-, and 5-year survival, respectively (Supplement Fig 4). In contrast, our 7-gene signature achieved markedly higher performance with AUCs of 0.979, 0.924, and 0.984 for 1, 3, and 5-year survival in Asian UM patients. This comparative analysis highlights the superior accuracy of our model and supports its potential as a population-specific prognostic tool. Nevertheless, the model demonstrated only moderate predictive ability when applied to TCGA data, exhibiting a lower level of performance than its implementation in the Asian cohort. This suggests that the model's performance may be influenced by population-specific factors, underscoring the necessity of additional validation across various ethnic groups.

The prognostic risk model established in this study, using seven pivotal genes (MMP2, LRAT, NOG, IHH, CDH18, MYH11, and SELE). Among the model's key genes, CDH18, a member of the cadherin family, has been linked to poor prognosis in UM and other cancers due to its involvement in macrophage infiltration. The strong association between CDH18 and macrophage M0 suggests its potential role in the transition of UM from

benign to malignant forms via modulating immunological responses [49]. MMP2 (Matrix Metalloproteinase 2) is recognized as a facilitator of epithelial-mesenchymal transition [50] and extracellular matrix remodeling [51], activities that enhance tumour cell motility and invasion [52]. Various cancers, particularly UM, have been associated with a poor prognosis due to increased MMP2 expression [35]. MYH11, a gene associated with muscle contraction and cellular migration [53], is correlated with a positive prognosis in UM [54]. LRAT (Lecithin Retinol Acyltransferase) modulates retinoid metabolism by promoting the esterification of retinol, playing a crucial role in the regulation of cell proliferation and differentiation in melanoma. A balanced LRAT expression correlates with improved clinical outcomes [55]. NOG (Noggin), a modulator of bone morphogenetic protein signaling, has been linked to metastasis, especially to bone [56]. SELE, linked to the suppression of melanoma metastasis, may serve as a potential therapeutic target [57]. In conclusion, our prognostic model offers significant insights into risk classification for Asian UM patients. Nonetheless, additional validation in a more extensive population is necessary to improve clinical applicability.

The study has several limitations. First, the significant age difference between cohorts may confound ethnic comparisons, underscoring the need for age-adjusted analyses in future studies. Although this is the largest transcriptome comparison of Asian and Caucasian UM to date, the relatively small sample size limits the generalizability of the findings. The bioinformatics results also lack experimental validation. Additionally, our direct tumor-to-tumor comparison approach, while necessary due to the absence of normal choroidal tissue data in the TCGA cohort, may conflate race-intrinsic differences with baseline expression variation between populations. Despite ComBat correction, batch effects between the TRACE and TCGA datasets may still introduce bias. This study also lacks prospective clinical validation in different populations. Finally, further investigation of genetic mutations enriched in Asian UM is warranted and will be addressed in future work. Together, these limitations highlight the need for additional research to validate and extend our findings.

Conclusions

In conclusion, this study highlights the differences in gene expression, immune microenvironment, and prognosis between Asian and Caucasian UM patients. Asian patients tend to have a more active immune environment, which may improve their response to immune checkpoint inhibitors. On the contrary, Caucasian patients show high levels of immunosuppression, which may impair the effect of immunotherapy. Future studies should further explore the molecular mechanisms behind these differences and improve the treatment strategies to improve the prognosis of UM patients worldwide.

Supplementary Information

The online version contains supplementary material available at https://doi.org/10.1186/s12886-025-04509-7.

Supplementary Material 1
Supplementary Material 2
Supplementary Material 3
Supplementary Material 4
Supplementary Material 5
Supplementary Material 6
Supplementary Material 7
Supplementary Material 8
Supplementary Material 9
Supplementary Material 10

Acknowledgements
We thank all authors for their contributions.

Author contributions
Design of the study (WBW, YL); Conduct of the study (YML, QY); Data collection (JTL， YNC, JYX, YXT); Analysis and interpretation (JTL, YNC, HWL); Manuscript preparation and review (ZXF, YL, WBW).

Funding
This work was supported by Capital Health Research and Development of Special (2024-1-2052); National Natural Science Foundation of China (82220108017, 82141128, 82101180); Beijing Natural Science Foundation (Z220012); Science & Technology Project of Beijing Municipal Science & Technology Commission (Z201100005520045); Sanming Project of Medicine in Shenzhen (SZSM202311018); The Fund for Beijing Science & Technology Development of TCM (BJZYYB-2023-17).

Data availability
The mRNA sequencing data and corresponding clinical information for 80 UM patients of the TCGA database were retrieved from https://tcga-data.nci.nih.gov/tcga/. Raw data of all normal choroid and UM samples were successfully uploaded on NCBI database and the data will be released at https://www.ncbi.nlm.nih.gov/sra/PRINA1091159 with publication. The datasets used and analyzed during the current study are available from the corresponding author on reasonable request. Researchers who require data from this study for research purposes can use it after obtaining the consent of the corresponding author (Wei WB, weiwenbintr@163.com) and signing a data access agreement.

Declarations

Ethics approval and consent to participate
This study adheres to the Helsinki Declaration and has received approval from the Ethics Committee of Beijing Tongren Hospital (Ethics Review Number: TRECKY2018-056). All patients signed informed consent for the use of tissue for research.

Consent for publication
Not applicable.

Competing interests
The authors declare no competing interests.

Author details
[1]Beijing Tongren Eye Center, Beijing Key Laboratory of Intraocular Tumor Diagnosis and Treatment, Beijing Ophthalmology & Visual Sciences Key Lab, Medical Artificial Intelligence Research and Verification Key Laboratory of the Ministry of Industry and Information Technology, Beijing Tongren Hospital, Capital Medical University, No. 1 Dongjiaominxiang, Dongcheng District, Beijing 100730, P. R. China
[2]Beijing Institute of Ophthalmology, Beijing Tongren Hospital, Capital Medical University, Beijing 100005, P. R. China
[3]Department of Ophthalmology, University of Ottawa, Ottawa, ON, Canada

Received: 14 May 2025 / Accepted: 6 November 2025
Published online: 02 December 2025

References

1. Jager MJ, Shields CL, Cebulla CM, Abdel-Rahman MH, Grossniklaus HE, Stern MH, Carvajal RD, Belfort RN, Jia R, Shields JA, et al. Uveal melanoma. Nat Rev Dis Primers. 2020;6(1):24.
2. Gill VT, Norrman E, Sabazade S, Karim A, Lardner E, Stålhammar G. Multiorgan involvement of dormant uveal melanoma micrometastases in postmortem tissue from patients without coexisting macrometastases. Am J Clin Pathol. 2023;160(2):164–74.
3. Hassel JC, Piperno-Neumann S, Rutkowski P, Baurain JF, Schlaak M, Butler MO, Sullivan RJ, Dummer R, Kirkwood JM, Orloff M, et al. Three-year overall survival with tebentafusp in metastatic uveal melanoma. N Engl J Med. 2023;389(24):2256–66.
4. Liu AW, Wei AZ, Maniar AB, Carvajal RD. Tebentafusp in advanced uveal melanoma: proof of principle for the efficacy of T-cell receptor therapeutics and bispecifics in solid tumors. Expert Opin Biol Ther. 2022;22(8):997–1004.
5. Carvajal RD, Sacco JJ, Jager MJ, Eschelman DJ, Olofsson Bagge R, Harbour JW, Chieng ND, Patel SP, Joshua AM, Piperno-Neumann S. Advances in the clinical management of uveal melanoma. Nat Rev Clin Oncol. 2023;20(2):99–115.
6. McLaughlin CC, Wu XC, Jemal A, Martin HJ, Roche LM, Chen VW. Incidence of noncutaneous melanomas in the U.S. Cancer. 2005;103(5):1000–07.
7. Hu DN, Yu GP, McCormick SA, Schneider S, Finger PT. Population-based incidence of uveal melanoma in various races and ethnic groups. Am J Ophthalmol. 2005;140(4):612–17.
8. Xu X, Wei WB, Li B, Gao F, Zhang Z, Jonas JB. Oncogenic GNAQ and GNA11 mutations in uveal melanoma in Chinese. PLoS One. 2014;9(10):e109699.
9. Bakhoum MF, Esmaeli B. Molecular characteristics of uveal melanoma: insights from the Cancer Genome Atlas (TCGA) project. Cancers (Basel). 2019;11(8).
10. Schneider B, Riedel K, Zhivov A, Huehns M, Zettl H, Guthoff RF, Jünemann A, Erbersdobler A, Zimpfer A. Frequent and yet unreported GNAQ and GNA11 mutations are found in uveal melanomas. Pathol Oncol Res. 2019;25(4):1319–25.
11. Pópulo H, Vinagre J, Lopes JM, Soares P. Analysis of GNAQ mutations, proliferation and MAPK pathway activation in uveal melanomas. Br J Ophthalmol. 2011;95(5):715–19.
12. Silva-Rodríguez P, Bande M, Fernández-Díaz D, Lago-Baameiro N, Pardo M, José Blanco-Teijeiro M, Domínguez F, Loidi L, Piñeiro A. Role of somatic mutations and chromosomal aberrations in the prognosis of uveal melanoma in a Spanish patient cohort. Acta Ophthalmol. 2021;99(7):e1077–89.
13. Psinakis F, Katseli A, Koutsandrea C, Frangia K, Florentin L, Apostolopoulou D, Dimakopoulou K, Papakonstantinou D, Georgopoulou E, Brouzas D. Uveal melanoma: GNAQ and GNA11 mutations in a Greek population. Anticancer Res. 2017;37(10):5719–26.
14. Wierenga APA, Brouwer NJ, Gelmi MC, Verdijk RM, Stern MH, Bas Z, Malkani K, van Duinen SG, Ganguly A, Kroes WGM, et al. Chromosome 3 and 8q aberrations in uveal melanoma show greater impact on survival in patients with light iris versus dark iris color. Ophthalmology. 2022;129(4):421–30.
15. Harbour JW, Onken MD, Roberson ED, Duan S, Cao L, Worley LA, Council ML, Matatall KA, Helms C, Bowcock AM. Frequent mutation of BAP1 in metastasizing uveal melanomas. Science. 2010;330(6009):1410–13.
16. Shields CL, Kaliki S, Furuta M, Fulco E, Alarcon C, Shields JA. American joint committee on cancer classification of uveal melanoma (anatomic stage) predicts prognosis in 7,731 patients: the 2013 Zimmerman Lecture. Ophthalmology. 2015;122(6):1180–86.
17. Robertson AG, Shih J, Yau C, Gibb EA, Oba J, Mungall KL, Hess JM, Uzunangelov V, Walter V, Danilova L, et al. Integrative analysis identifies four molecular and clinical subsets in uveal melanoma. Cancer Cell. 2017;32(2):204–20.e215.
18. Harbour JW, Correa ZM, Schefler AC, Mruthyunjaya P, Materin MA, Ta A, Skalet AH, Reichstein DA, Weis E, Kim IK, et al. 15-Gene expression profile and prame as integrated prognostic test for uveal melanoma: first report of collaborative ocular oncology group study No.2 (COOG2.1). J Clin Oncol. 2024;42(28):3319–29.
19. Suwajanakorn D, Lane AM, Go AK, Hartley CD, Oxenreiter M, Wu F, Gragoudas ES, Sullivan RJ, Montazeri K, Kim IK. Impact of gene expression profiling on diagnosis and survival after metastasis in patients with uveal melanoma. Melanoma Res. 2024;34(4):319–25.
20. Yu G, Wang LG, Han Y, He QY. clusterProfiler: an R package for comparing biological themes among gene clusters. Omics. 2012;16(5):284–87.
21. Szklarczyk D, Gable AL, Lyon D, Junge A, Wyder S, Huerta-Cepas J, Simonovic M, Doncheva NT, Morris JH, Bork P, et al. String v11: protein-protein association networks with increased coverage, supporting functional discovery in genome-wide experimental datasets. Nucleic Acids Res. 2019;47(D1):D607–d613.
22. Shannon P, Markiel A, Ozier O, Baliga NS, Wang JT, Ramage D, Amin N, Schwikowski B, Ideker T. Cytoscape: a software environment for integrated models of biomolecular interaction networks. Genome Res. 2003;13(11):2498–504.
23. Chin CH, Chen SH, Wu HH, Ho CW, Ko MT, Lin CY. cytoHubba: identifying hub objects and sub-networks from complex interactome. BMC Syst Biol. 2014;8(Suppl 4):S11.
24. Friedman J, Hastie T, Tibshirani R. Regularization paths for generalized linear models via coordinate descent. J Stat Softw. 2010;33(1):1–22.
25. Newman AM, Liu CL, Green MR, Gentles AJ, Feng W, Xu Y, Hoang CD, Diehn M, Alizadeh AA. Robust enumeration of cell subsets from tissue expression profiles. Nat Methods. 2015;12(5):453–57.
26. Yoshihara K, Shahmoradgoli M, Martínez E, Vegesna R, Kim H, Torres-Garcia W, Treviño V, Shen H, Laird PW, Levine DA, et al. Inferring tumour purity and stromal and immune cell admixture from expression data. Nat Commun. 2013;4:2612.
27. Maeser D, Gruener RF, Huang RS. OncoPredict: an R package for predicting in vivo or cancer patient drug response and biomarkers from cell line screening data. Brief Bioinform. 2021;22(6).
28. Thorsson V, Gibbs DL, Brown SD, Wolf D, Bortone DS, Ou Yang TH, Porta-Pardo E, Gao GF, Plaisier CL, Eddy JA, et al. The immune landscape of cancer. Immunity. 2018;48(4):812–30.e814.
29. Liu XL, Run-Hua Z, Pan JX, Li ZJ, Yu L, Li YL. Emerging therapeutic strategies for metastatic uveal melanoma: targeting driver mutations. Pigment Cell Melanoma Res. 2024;37(3):411–25.
30. Katopodis P, Khalifa MS, Anikin V. Molecular characteristics of uveal melanoma and intraocular tumors. Oncol Lett. 2021;21(1):9.
31. Wei AZ, Maniar AB, Carvajal RD. New targeted and epigenetic therapeutic strategies for the treatment of uveal melanoma. Cancer Gene Ther. 2022;29(12):1819–26.
32. Kassumeh S, Arrow S, Kafka A, Luft N, Priglinger SG, Wolf A, Eibl-Lindner K, Wertheimer CM. Pharmacological drug screening to inhibit uveal melanoma metastatic cells either via EGF-R, MAPK, mTOR or PI3K. Int J Ophthalmol. 2022;15(10):1569–76.
33. Park JJ, Hamad SA, Stewart A, Carlino MS, Lim SY, Rizos H. PKC-independent PI3K signalling diminishes PKC inhibitor sensitivity in uveal melanoma. Oncogenesis. 2024;13(1):9.
34. Li Y, Xiong C, Wu LL, Zhang BY, Wu S, Chen YF, Xu QH, Liao HF. Tumor subtypes and signature model construction based on chromatin regulators for better prediction of prognosis in uveal melanoma. Pathol Oncol Res. 2023;29:1610980.
35. Wang T, Zhang Y, Bai J, Xue Y, Peng Q. MMP1 and MMP9 are potential prognostic biomarkers and targets for uveal melanoma. BMC Cancer. 2021;21(1):1068.
36. Jehs T, Faber C, Juel HB, Bronkhorst IH, Jager MJ, Nissen MH. Inflammation-induced chemokine expression in uveal melanoma cell lines stimulates monocyte chemotaxis. Invest Ophthalmol Vis Sci. 2014;55(8):5169–75.
37. Clarijs R, Schalkwijk L, Ruiter DJ, de Waal Rm. EMAP-II expression is associated with macrophage accumulation in primary uveal melanoma. Invest Ophthalmol Vis Sci. 2003;44(5):1801–06.
38. Qin Y, Bollin K, de Macedo MP, Carapeto F, Kim KB, Roszik J, Wani KM, Reuben A, Reddy ST, Williams MD, et al. Immune profiling of uveal melanoma

identifies a potential signature associated with response to immunotherapy. J Immunother Cancer. 2020;8(2).
39. Singh L, Singh MK, Kenney MC, Jager MJ, Rizvi MA, Meel R, Lomi N, Bakhshi S, Sen S, Kashyap S. Prognostic significance of PD-1/PD-L1 expression in uveal melanoma: correlation with tumor-infiltrating lymphocytes and clinicopathological parameters. Cancer Immunol Immunother. 2021;70(5):1291–303.
40. He YG, Mayhew E, Mellon J, Niederkorn JY. Expression and possible function of IL-2 and IL-15 receptors on human uveal melanoma cells. Invest Ophthalmol Vis Sci. 2004;45(12):4240–46.
41. Repp AC, Mayhew ES, Apte S, Niederkorn JY. Human uveal melanoma cells produce macrophage migration-inhibitory factor to prevent lysis by nk cells. The J Immunol. 2000;165(2):710–15.
42. Hoefsmit EP, Rozeman EA, Van TM, Dimitriadis P, Krijgsman O, Conway JW, Pires da Silva I, van der Wal JE, Ketelaars SLC, Bresser K, et al. Comprehensive analysis of cutaneous and uveal melanoma liver metastases. J Immunother Cancer. 2020;8(2).
43. Yang H, Brackett CM, Morales-Tirado VM, Li Z, Zhang Q, Wilson MW, Benjamin C, Harris W, Waller EK, Gudkov AV, et al. The Toll-like receptor 5 agonist entolimod suppresses hepatic metastases in a murine model of ocular melanoma via an nk cell-dependent mechanism. Oncotarget. 2016;7(3):2936–50.
44. Zhang Z, Su J, Li L, Du W. Identification of precise therapeutic targets and characteristic prognostic genes based on immune gene characteristics in uveal melanoma. Front Cell Dev Biol. 2021;9:666462.
45. Onken MD, Worley LA, Char DH, Augsburger JJ, Correa ZM, Nudleman E, Tm A, Altaweel MM, Bardenstein DS, Finger PT, et al. Collaborative ocular oncology group report number 1: prospective validation of a multi-gene prognostic assay in uveal melanoma. Ophthalmology. 2012;119(8):1596–603.
46. Bk W, Siegel JJ, Alsina KM, Johnston L, Sisco A, LiPira K, Selig SM, Hovland PG. Uveal melanoma patient attitudes towards prognostic testing using gene expression profiling. Melanoma Manag. 2022;9(3):Mmt62.
47. Aaberg TM, Covington KR, Tsai T, Shildkrot Y, Plasseraud KM, Alsina KM, Oelschlager KM, Monzon FA. Gene expression profiling in Uveal melanoma: five-year prospective outcomes and meta-analysis. Ocul Oncol Pathol. 2020;6(5):360–67.
48. Meng S, Zhu T, Fan Z, Cheng Y, Dong Y, Wang F, Wang X, Dong D, Yuan S, Zhao X. Integrated single-cell and transcriptome sequencing analyses develops a metastasis-based risk score system for prognosis and immunotherapy response in uveal melanoma. Front Pharmacol. 2023;14:1138452.
49. Song X, Na R, Peng N, Cao W, Ke Y. Exploring the role of macrophages in the progression from atypical hyperplasia to endometrial carcinoma through single-cell transcriptomics and bulk transcriptomics analysis. Front Endocrinol (Lausanne). 2023;14:1198944.
50. Hou Q, Han S, Yang L, Chen S, Chen J, Ma N, Wang C, Tang J, Chen X, Chen F, et al. The interplay of microRNA-34a, LGR4, EMT-associated factors, and MMP2 in regulating uveal melanoma cells. Invest Ophthalmol Vis Sci. 2019;60(13):4503–10.
51. Lai K, Conway RM, Crouch R, Jager MJ, Madigan MC. Expression and distribution of MMPs and TIMPs in human uveal melanoma. Exp Eye Res. 2008;86(6):936–41.
52. Rossi S, Cordella M, Tabolacci C, Nassa G, D'Arcangelo D, Senatore C, Pagnotto P, Magliozzi R, Salvati A, Weisz A, et al. TNF-alpha and metalloproteases as key players in melanoma cells aggressiveness. J Exp Clin Cancer Res. 2018;37(1):326.
53. Wang C, Zhao Y, Zhang S, Du M, He G, Tan S, Li H, Zhang D, Cheng L. Single-cell rna sequencing reveals the heterogeneity of MYH11+ tumour-associated fibroblasts between left-sided and right-sided colorectal cancer. J Cell Mol Med. 2024;28(18):e70102.
54. Nie MJ, Pan XT, Tao HY, Xu MJ, Liu SL, Sun W, Wu J, Zou X. Clinical and prognostic significance of MYH11 in lung cancer. Oncol Lett. 2020;19(6):3899–906.
55. Amann PM, Czaja K, Bazhin AV, Rühl R, Skazik C, Heise R, Marquardt Y, Eichmüller SB, Merk HF, Baron JM. Knockdown of lecithin retinol acyltransferase increases all-trans retinoic acid levels and restores retinoid sensitivity in malignant melanoma cells. Exp Dermatol. 2014;23(11):832–37.
56. Tarragona M, Pavlovic M, Arnal-Estapé A, Urosevic J, Morales M, Guiu M, Planet E, González-Suárez E, Gomis RR. Identification of nog as a specific breast cancer bone metastasis-supporting gene. J Biol Chem. 2012;287(25):21346–55.
57. Liu LP, Liu N, Zhang HN, Li D. Exploring and validating the metastasis mechanism of pathenolide interfering with cutaneous melanoma through er stress-dependent apoptosis based on the network pharmacology. Phytochem Anal. 2023;34(7):745–54.

Publisher's Note